Descriptions and Analyses of Guest Cavity Size and Shape in a New Family of Helical Tubuland Inclusion Crystals

Ian G. Dance,* Roger Bishop, and Marcia L. Scudder
School of Chemistry, University of New South Wales, Kensington, New South Wales 2033, Australia

The crystal structures of *exo*-2,*exo*-6-dihydroxy-2,6-dimethylbicyclo[3.3.1]nonane, *syn*-2,*syn*-7-dihydroxy-2,7-dimethyltricyclo[4.3.1.1^{3,8}]undecane, *anti*-2,*anti*-7-dihydroxy-2,7-dimethyltricyclo-[4.3.1.1^{3,8}]undecane, and *syn*-2,*syn*-8-dihydroxy-2,8-dimethyltricyclo[5.3.1.1^{3,9}]dodecane, four geometrically different instances of the helical tubuland inclusion lattice, are analysed in terms of the structural variables of the host molecules and the lattice, which allow substantial variations in the sizes and shapes of the inclusion cavities. The cavity dimensions are described in detail.

In the preceding paper[1] we described the syntheses and crystal structure determinations for the four related diols *exo*-2,*exo*-6-dihydroxy-2,6-dimethylbicyclo[3.3.1]nonane (**1**), *syn*-2,*syn*-7-dihydroxy-2,7-dimethyltricyclo[4.3.1.1^{3,8}]undecane (**2**), *anti*-2,*anti*-7-dihydroxy-2,7-dimethyltricyclo[4.3.1.1^{3,8}]undecane (**3**), and *syn*-2,*syn*-8-dihydroxy-2,8-dimethyltricyclo[5.3.1.1^{3,9}]-dodecane (**4**). All four compounds crystallise in the chiral space group $P3_121$ (or its enantiomer),† with the helical tubuland[2] inclusion structure type in which the diol host molecules connect spiral spines of hydrogen bonds. This new tubuland inclusion structure differs distinctly from that formed by urea and thiourea, in that the host hydrogen bonds are localised and isolated from the guest tubes, which are lined with hydrocarbon groups only.

A significant result is that, even though the diols (**1**)—(**4**) adopt a lattice structure with the same symmetry, and the host molecules are virtually identical with respect to intramolecular separation and orientation of the two OH functions, the dimensions of the host lattice vary substantially (unit-cell volumes 853—1 150 Å^3) and the projected cross-sections of the tubes available to guest species change dramatically in shape and area (4.7 to 34.7 Å^2). These results establish the feasibility of controlled and selective guest inclusion in a host lattice of constant symmetry but variable size and shape, through modification of the host molecule. There occur in the crystals of (**1**)—(**4**) subtle influences of the host molecular shape on the dimensions of the host lattice, and, through variations of these dimensions and the variable intrusion of hosts into the guest cavity, pronounced influences on the sizes and shapes available to potential guest species.

The purposes of this paper are (i) to delineate the structural variables in this helical tubuland lattice type, (ii) to identify the locations and causes of the subtle influences of host molecular dimensions on guest cavity size and shape, and (iii) to describe three-dimensional details of the shapes and capacities of the guest cavities. Clear understanding of these three facets is necessary for rational design of further helical tubuland host lattices in this class. The first section below describes the lattice and defines its geometrical variables, the second section identifies the causes and effects, and the third section provides and analyses stereoscopic views of the van der Waals surfaces of the host structures.

Definitions of Fundamental Attributes and Variables of the Helical Tubuland Structure Type.—The space group of the lattice is $P3_121$ (or its enantiomorph $P3_221$), in which there are three-fold screw axes parallel to c at x,y = 0,0; 1/3,2/3; and 2/3,1/3. There are six two-fold axes perpendicular to c: two are parallel to a at z = 1/3,5/6; two are parallel to b at z = 1/6,2/3; and two are parallel to the ab diagonal at z = 0,1/2. Figure 1 is a diagrammatic representation of the key elements of the structure. Diol molecules, which straddle the two-fold axes at z = 1/6, 1/2, and 5/6 only, are hydrogen-bonded around a tube in the spiral sequence (A) such that each diol functions as a

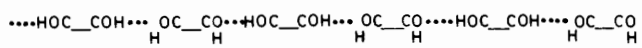

(A)

C—C represents diol core

double hydrogen donor or a double hydrogen acceptor in the sequence. There is a translation of $c/3$ at each hydrogen bond, and a complete turn of each spiral chain contains six diol molecules. Therefore the pitch of each chain is $2c$, and, as a consequence of the c repetition of diol molecules, the host spiral is comprised of *two* separate helical chains of the above type, without *direct* hydrogen bond linkage between the helices. The double helix which envelops a tube of (**1**) is shown diagrammatically in exaggerated perspective in Figure 2. The hydrogen-bonded spines are single helices of pitch c.

The asymmetric unit of the host structure in $P3_121$ is half a diol molecule, with one acceptor and one donor hydrogen bond. The asymmetric volume of a tube is a 60° sector (height c) subtended by a vertical half of a *syn* face and the contiguous vertical half of an *anti* face (see later).

In this space-group symmetry each diol molecule has two degrees of freedom, namely twist about and displacement along its two-fold axis. Both these changes affect the dimensions of the hydrogen bonds and the dimensions of the tubular cavities. It is useful to invoke the imagery of the wire coil mattress in description of the essential components of the lattice structure, which are the spines of hydrogen bonds and the rigid diol molecules which interconnect them through the O–C bonds which radiate from the spines. The coiled springs (representing the hydrogen-bonded spines) are interconnected in hexagonal array by stiff linkages (the diol molecules) with flexibility at the linkage-coil connections (the C–OH · · · O hydrogen bonds). This analogy illustrates one form of variability of the lattice structure, namely compression or elongation of the spines (springs), concomitant with twisting of the diol molecules about their two-fold axes.

The role of the diol as rigid connector between the hydrogen-

† In the case of (**3**) there is evidence for lower diffraction symmetry, but the structural cause of this has not yet been identified.

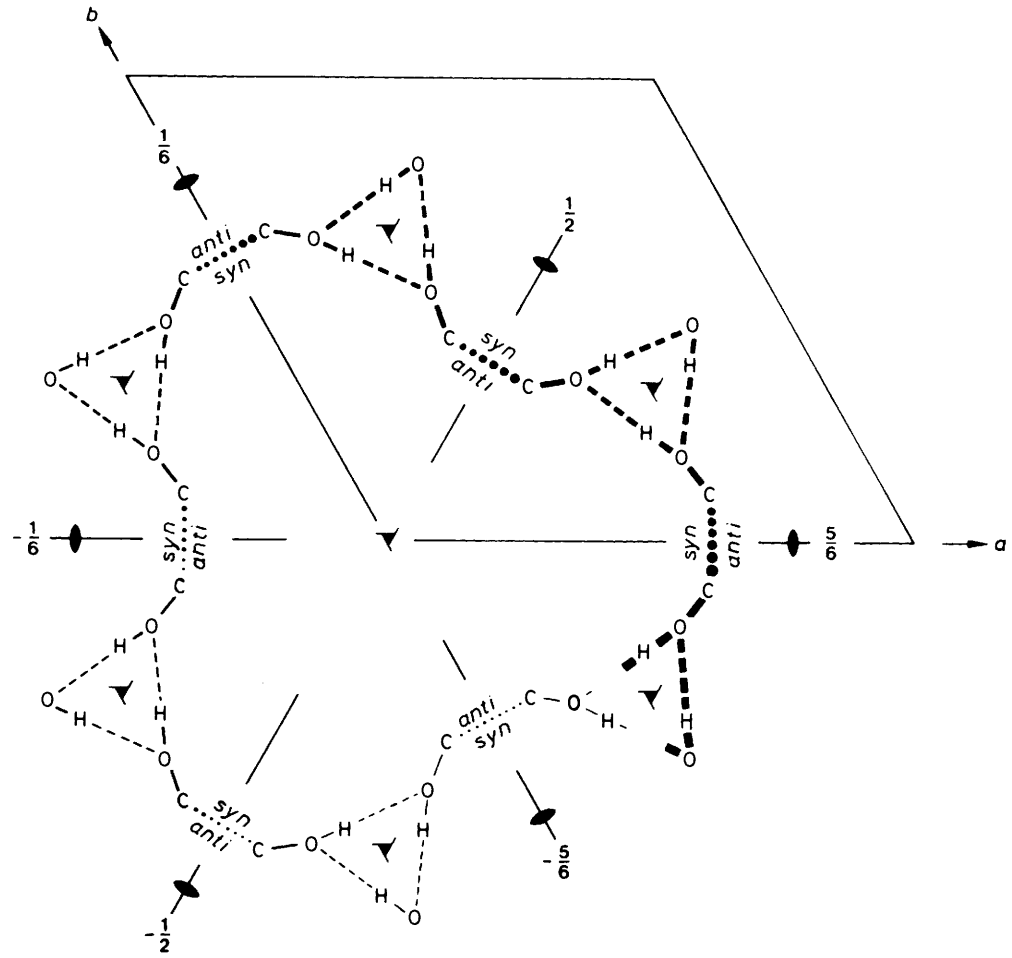

Figure 1. Diagrammatic representation of the sequence of hydrogen-bonded diol molecules (denoted HOC···COH) comprising one turn of the spiral (pitch 2*c*) around the tube. Lateral two-fold axes at the *z* co-ordinates marked bisect the diol molecules. The hexagonal array of hydrogen-bond spines (each with three-fold screw symmetry), and the alternation of *syn* and *anti* faces of the host diols around the canal are shown. In the space group $P3_121$ there are additional lateral two-fold axes displaced by $z = 1/2$ from those shown

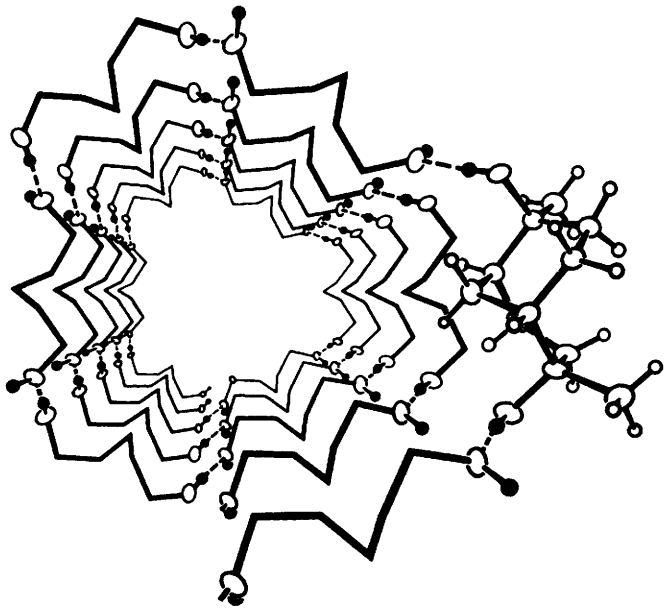

Figure 2. Exaggerated perspective view of the helical sequence of hydrogen-bonded diol molecules in one tube of (**1**): all except one diol molecule are represented diagrammatically as the bridge linkage of the two OH groups

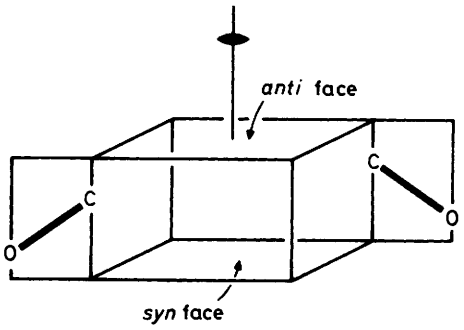

Figure 3. Diagrammatic representation of key characteristics of the diol molecule, with two-fold symmetry, C–O bonds in parallel planes, and faces *syn* and *anti* to the pair of C–O bonds

bonded spines is to provide two C–OH functions in fixed orientation. Relative to the rigid diol molecule the essential geometrical characteristics of the pair of C–O bonds are shown diagrammatically in Figure 3. The C–O bonds lie in opposing planes parallel to the two-fold axis of the molecule, and are directed at an angle of approximately 50° to a plane perpendicular to the molecular two-fold axis. Consequently the host molecule possesses different two-fold faces which are *syn*

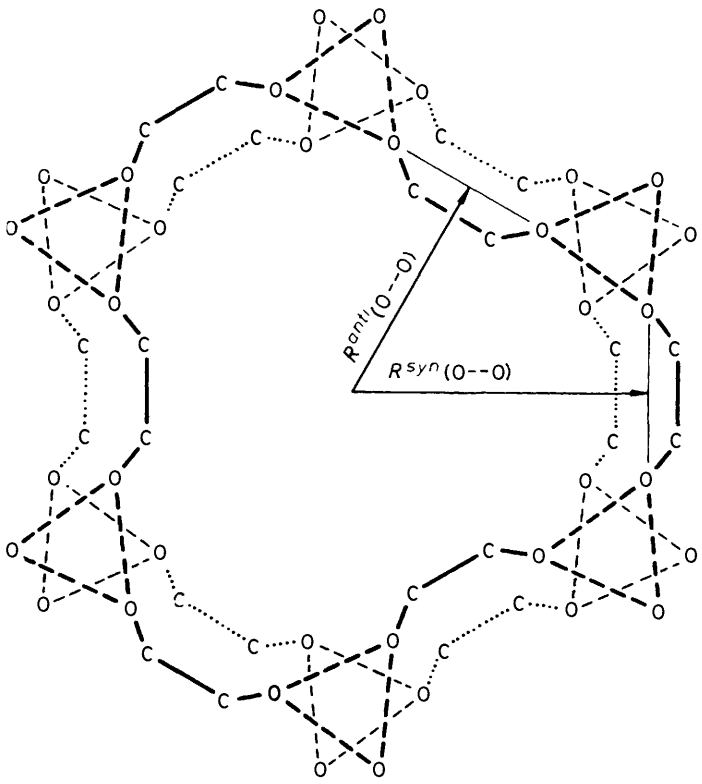

Figure 4. Diagrammatic representation of the variations in lattice structure and tube shape dependent on the variable displacement of diol molecules along their two-fold axes in space group $P3_121$. Two alternative dispositions of the diol molecules (depicted simply as O–C - - - C–O) and the projected hydrogen-bonded spines are shown, and differentiated by thicker and thinner lines. The rotational orientations of the triangular projections of the hydrogen-bond spines depend on the ratio of the two variables R^{syn}(O - - - O) and R^{anti}(O - - - O) (marked for the thicker disposition of diol molecules), which are the lengths of the perpendiculars from the O - - - O vector to the tube axis

and *anti* relative to the C–O bonds.* When the diol molecules are included to connect the spines, the helical chain sequence around each tube presents *syn* and *anti* faces alternately towards the centre of the tube, as shown in Figure 1. There is only one type of tube in the structure, with a size and shape which is influenced by *both* the *syn* and *anti* portions of the host molecule.

The contra-molecular distances between the two C–O functions, and the C - - - C–O angles, are virtually invariant through the four host molecules.[1] The one significant difference occurs in the O–C - - - C′–O′ torsion angle, which is 73.5 and 79.0° in (**1**) and (**3**), and 94.3 and 97.2° in (**2**) and (**4**), respectively.

The displacements of the diol molecules along the two-fold axes are expressed by the radii R^{syn}(O - - - O), R^{anti}(O - - - O) defined in Figure 4 as the distances of the intramolecular O - - - O vectors from the tube axis through the *syn* and *anti* faces. Note that R^{syn}(O - - - O) + R^{anti}(O - - - O) = a. The absolute values of R(O - - - O) give the sizes of the tubes, divorced from any of the variable effects due to the bridging

* The descriptions *syn* and *anti* in the names of the host molecules refer to the OH functions relative to the larger of the bridges across the molecular two-fold axis. Here *syn* and *anti* distinguish the host molecule faces, referenced to the C–O bond directions.

Table 1. Values (Å) of radii defining the positions of host molecules along two-fold axes

Radius	(1)	(2)	(3)	(4)
R^{anti}(O - - - O)	5.57	6.28	5.34	6.85
R^{syn}(O - - - O)	6.60	6.91	6.56	6.89
R^{anti}(C - - - C)	3.85	4.65	3.60	5.31
R^{syn}(C - - - C)	6.72	6.88	6.64	6.84

atoms of the diol hosts, while the relative values of R^{syn}(O - - - O) and R^{anti}(O - - - O) correlate with rotational twists of the triangular projections of the spines, as illustrated in Figure 4. Variations in R^{syn}(O - - - O)/R^{anti}(O - - - O) affect also the directions of the hydrogen bonds relative to the host molecule.

A final definition, pertinent to the intrusion of diol bridges into the tube, refers to the radius from the centre of the tube to the intramolecular vector connecting the pair of bridgehead carbon atoms which support the bridge. The bridgehead vectors are C(2) - - - C(2′) and C(4) - - - C(4′) in the labelling scheme (**B**) common to the four structures. The radii are R^{syn}(C - - - C)

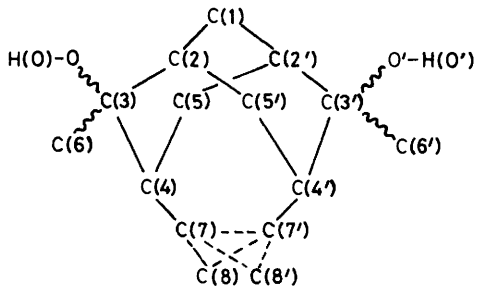

(**B**)

and R^{anti}(C - - - C) for bridges on the *syn* and *anti* faces of the host molecules.

Comparison of the Lattice Structures.—The lattice dimensions vary in a, not c. The hexagonal area between the spines therefore varies in the ratios (a^2) 1.00:1.18:0.96:1.28 for (**1**), (**2**), (**3**), and (**4**), respectively. Values of the radii R(O - - - O) describing the positions of the host molecules along the two-fold axes are listed in Table 1, and reveal that the major variations occur in R^{anti}(O - - - O). Whereas the range of values of R^{syn}(O - - - O) is 5% of the mean value of 6.74 Å, the R^{anti}(O - - - O) radii are variable over a range of 1.51 Å which is 25% of their mean. There is a concomitant variation in R^{anti}(O - - - O)/R^{syn}(O - - - O) and the rotational orientations of the projected hydrogen bond triangles. This ratio is largest in (**4**), at 0.99 (the projected hydrogen bonds are almost parallel to the lattice axes), and decreases through 0.91 in (**2**), 0.84 in (**1**), to 0.81 in (**3**). The variable orientations of the hydrogen-bond triangles, clearly apparent in Figure 5, therefore are due to changes in R^{anti}(O - - - O).

The twist of each diol molecule about its two-fold axis can be expressed in terms of the difference (Å) between z co-ordinates of the two oxygen atoms: these differences are 1.39, 0.87, 1.42, and 1.62 Å for (**1**), (**2**), (**3**), and (**4**), respectively. The angles of inclination of the C–O bonds to the planes normal to the spine axes are 13, 21, 14, and 8°, respectively: the differences here are of minor significance.

The different rotations of the projected hydrogen bonds about the spine axis, without change in the pitch of the spiral,

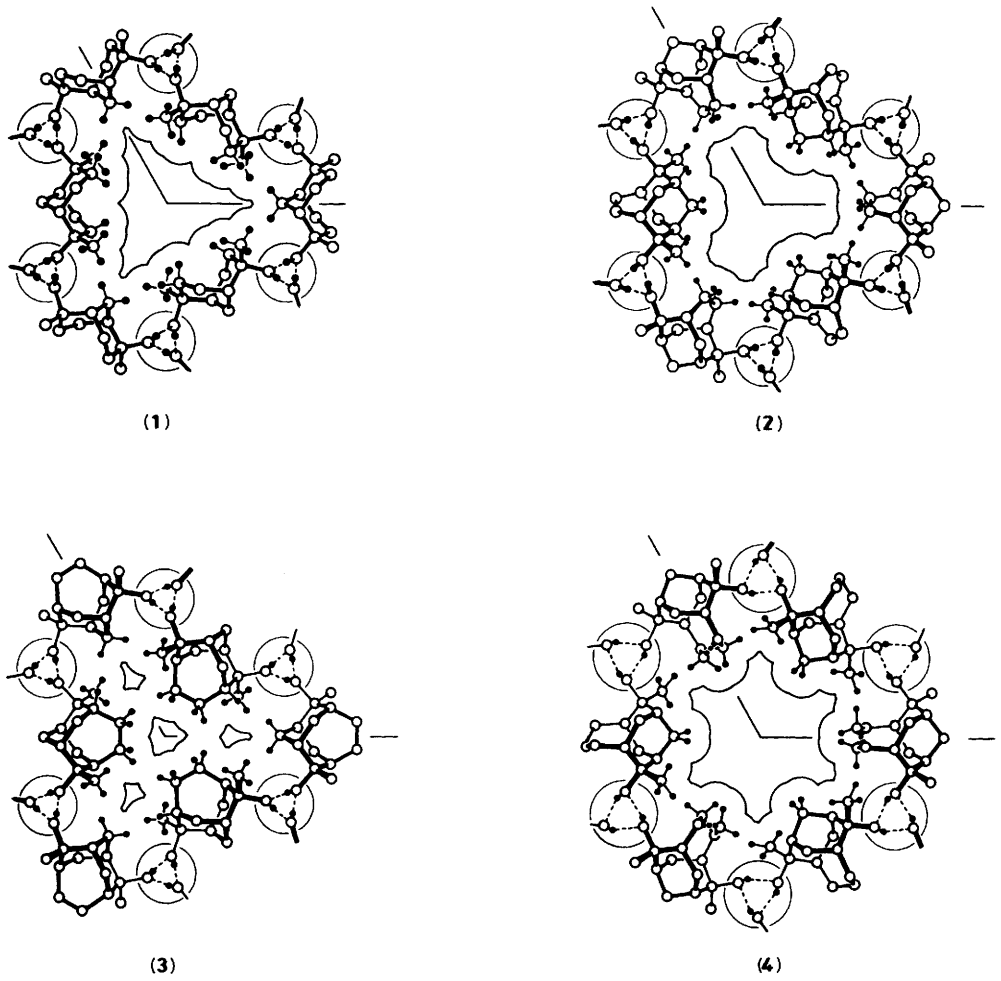

Figure 5. Comparative projections along the *c* axis of the diol molecules and the tubes they enclose in (**1**)—(**4**). Bond thickening signifies depth in individual molecules only, because the helical characteristic is absent from these projections of the lattice. The tube boundaries are marked as the intersecting projected van der Waals spheres of the hydrogen atoms which line the tube. All four diagrams are presented on the same scale. Significant hydrogen atoms are marked as filled circles, and the spines are circled

Table 2. Hydrogen-bond dimensions[a] for (**1**)—(**4**)

Dimension	(1)	(2)		(3)		(4)
O–H (Å)	0.67(5)	0.76(5)	0.81(6)	0.85(5)	0.89(5)	0.87(6)
C–O–H (°)	114(3)	109(2)	105(3)	114(3)	109(3)	109(3)
O – – – O_A[b] (Å)	2.810(2)	2.981(2)	2.838(4)	2.839(3)	2.833(3)	3.084(2)
C–O – – – O_A (°)	108.4(1)	108.0(1)	106.6(2)	106.4(2)	106.4(1)	112.1(1)
O–H – – – O_A (°)	170(4)	172(4)	170.(4)	162(4)	171(4)	173(4)
C–O – – – O_D (°)	128.2(2)	130.4(2)	132.3(2)	132.5(2)	132.8(2)	120.2(2)
O_A – – – O – – – O_D (°)	122.33(9)	113.37(7)	120.8(1)	120.9(1)	120.7(1)	111.48(6)

[a] See diagram (C) for definitions. [b] O – – – O_D is equal to O – – – O_A except for (**3**).

require variation in the direction of approach of the C–OH functions to the hydrogen-bond spines, and in the geometry of hydrogen bonding. The local hydrogen-bonding environment is shown in diagram (C), and distances and angles are presented in Table 2. In all cases the acceptor O_A towards which the OH bond is directed is nearer to the *syn* face of the diol molecule, as shown. The C–O–H, C–O – – – O_A and O–H – – – O_A angles are all close to ideal values, and there is no evident strain in the hydrogen bonding. The hydrogen atom is located at the better of the two alternative positions along each O – – – O con-

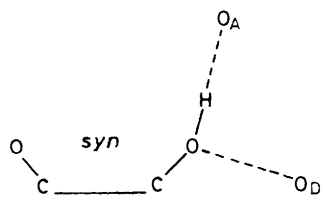

(C)

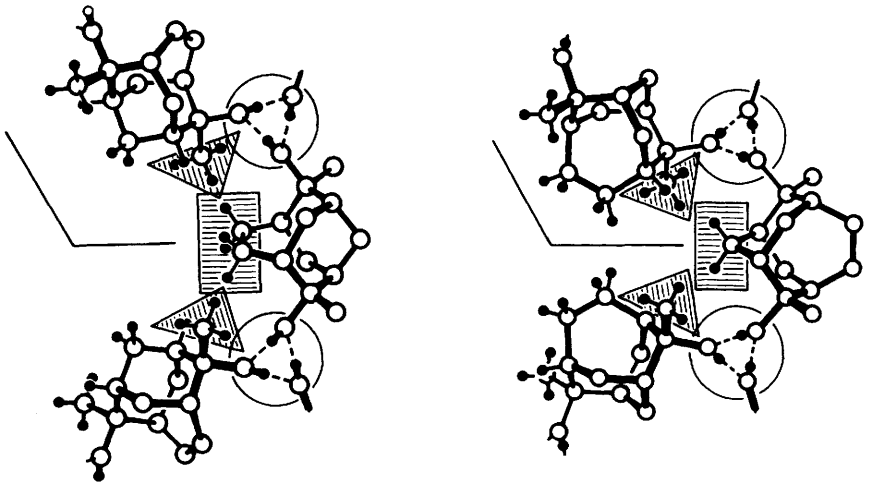

Figure 6. Projections of structures (**2**) and (**3**) along the *c* axis showing the *syn* bridge (cross-hatched rectangle) on the tube *syn* wall and its differing proximity to the methyl substituents (cross-hatched triangles) on the flanking *anti* walls

nection, that is the C–O(H) - - - O_A angles are closer to tetrahedral, 106—112°, and the C–O - - - (H)O_D angles are 120—133° in the four structures. The methyl substituent does not interfere with the hydrogen bonding. The main difference amongst the four structures is that in (**2**) and (**4**) the O - - - O distance is longer, by *ca.* 0.15 Å in (**2**) and *ca.* 0.25 Å in (**4**), and the O - - - O - - - O angle is 10° smaller. According to the preceding arguments this effect can be traced to the increased R^{anti}(O - - - O) in (**2**) and (**4**). Because the elongation of the hydrogen bonds in (**2**) and (**4**) is clearly a weakening, it can be concluded that the increased R^{anti}(O - - - O) in (**2**) and (**4**) have affected the hydrogen bonding, and not *vice versa.*

We believe that the cause of the increased R^{anti}(O - - - O) in (**2**) and (**4**), and thus the cause of all other differences described here, is repulsion between the diol methyl substituents and the *syn* bridge of adjacent diols. Two characteristics of the *syn* bridge in (**2**) and (**4**) contribute to this influence, namely the steep inclination of the bridge almost parallel to the tube axis, and the increased length, ethano in (**2**), propano in (**4**), to be compared with the methano bridge in (**1**) and (**3**). Consequently the ends of the *syn* bridge are close to the methyl substituents of the contiguous diols in the spiral chain. This inter-diol contact is shown diagrammatically on Figure 6. This repulsive interference arises because the *syn* bridges in (**2**) and (**4**) are sufficiently large to occupy most of the *syn* face of the tube wall (see later, and also Figure 9), and to exclude the methyl substituents which protrude from the adjacent *anti* walls of the tube. Relief of this interference is effected by an increase of R^{anti}(O - - - O), which decreases the intrusion of the methyl groups upon the *syn* wall of the tube. Thus van der Waals contact between hydrogen atoms of the methyl substituent and the ethano *syn* bridge in (**2**) occurs at 2.68 Å [H(3)C(6) - - - H(1)C(7)], requiring R^{anti}(O - - - O) = 6.28 Å: in (**4**) contacts between methyl- and propano-*syn* bridge hydrogen atoms are 2.45 Å [H(3)C(6) - - - H(2)C(7)], 2.53 Å [H(2)C(6) - - - H(2)C(8)], 2.69 Å [H(3)C(6) - - - H(1)C(7)], and 2.71 Å [H(3)C(6) - - - H(1A)C(7)], requiring a larger value of R^{anti}(O - - - O) = 6.85 Å. In (**1**) and (**3**) smaller values of R^{anti}(O - - - O) (5.57 and 5.34 Å) allow similar contacts between methyl hydrogen atoms and *syn* bridge methano hydrogen atoms, *viz.* 2.72 Å [H(3)C(6) - - - HC(1)] for (**1**) and 2.62 Å [H(3)C(6) - - - HC(1)] for (**3**). Note that in this crystal structure type the ethano bridge in (**3**) cannot be compared with the ethano bridge in (**2**): in (**3**) it is on the *anti* face, and is inclined transverse to the tube axis, with no possible interference to the methyl substituents.

Shapes and Capacities of the Tubular Cavities.—The sizes and shapes of the tubular cavities are influenced directly and indirectly by several factors. The first, noted already, is that the areas between the spine networks vary in the ratios 1.00:1.18:0.96:1.28 for (**1**), (**2**), (**3**), and (**4**), an indirect consequence of the identity of the *syn* bridge. A more useful expression of this is in the location of the foundations of the bridges which constitute the walls of the tube, defined by the radii *R*(C - - - C). Table 1 shows that R^{anti}(C - - - C) is always less than R^{syn}(C - - - C) [by 2.87 and 3.04 in (**1**) and (**3**), 2.23 Å in (**2**), and 1.53 Å in (**4**)], and that R^{anti}(C - - - C) is the more variable. The more evident influence on the tube dimensions is the identity (or absence) of the bridges on these foundations. The combination of these factors accounts for the very variable unobstructed cross-sectional shapes and sizes of the tube. We now examine the indentations in the tube walls, not apparent in the projection views, but which enlarge the accommodation for guest species. The internal surfaces of the tubes are defined by the intersections of the van der Waals spheres (radius 1.2 Å) of the hydrogen atoms which line the walls. These van der Waals surfaces are presented with the stereoviews in Figures 7—9. For each crystal structure three stereoviews are presented: one (in Figure 7) is a view of the spiral along the *c* axis; a second (in Figure 8) is a view from inside the tube towards the *syn* wall, flanked on both sides with molecules presenting an *anti* face to the tube; and the third (in Figure 9) is towards the *anti* wall with flanking *syn* walls.

The principal result provided by these stereodiagrams is that the indentations in the walls are substantial and generally able to accommodate at least CH_3 or CH_2 groups in a manner which is not revealed by the projection diagrams. In fact the differences amongst the four structures are exaggerated by the projection diagrams, and the *shapes* of the tube walls in the four structures have many similarities. For instance, comparison of (**3**) and (**2**) in Figure 8 shows a similar openness of wall structure not revealed by the projections of Figure 5. The stereodiagrams also manifest the overall larger dimensions of the canal lattices in (**2**) and (**4**).

In all structures the *anti* wall is more exposed to the tube than

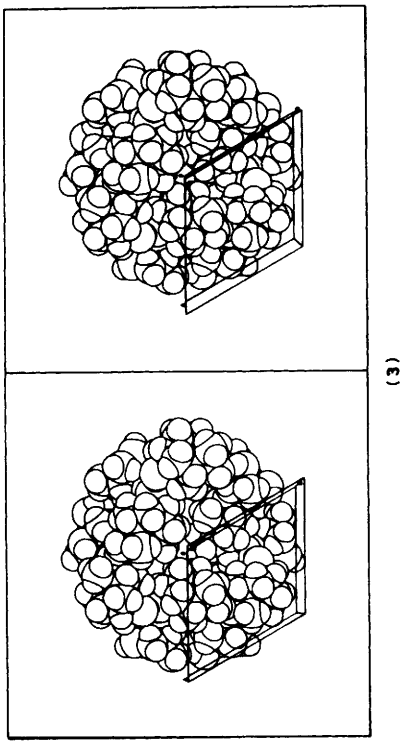

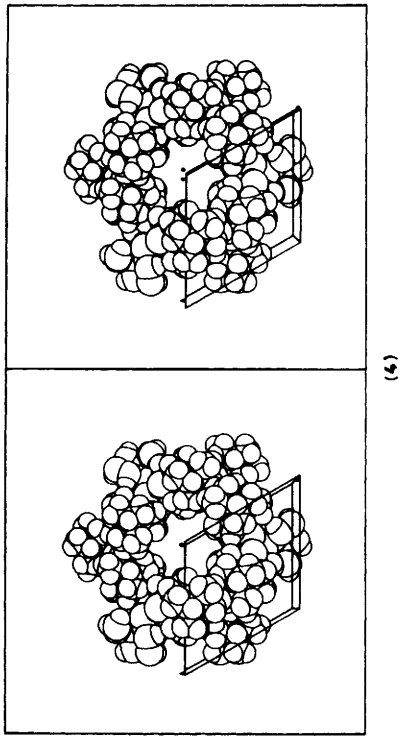

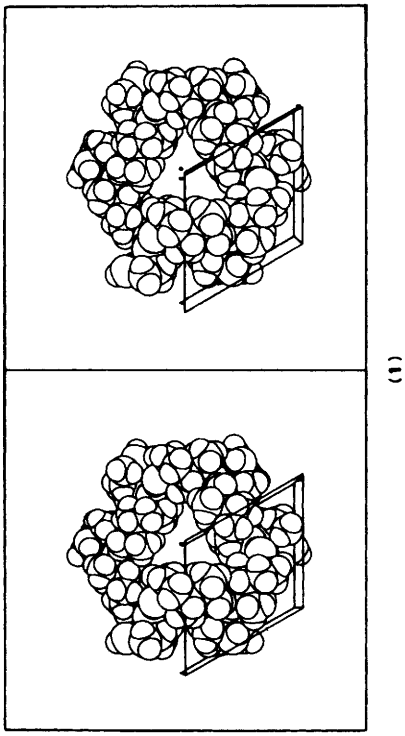

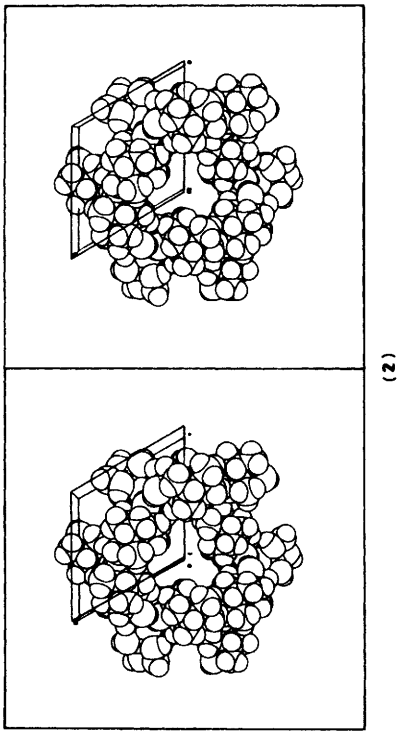

Figure 7. Stereopair pictures of the crystal structures of (1)—(4) at van der Waals volume, showing a complete spiral of the tube viewed along the tube axis

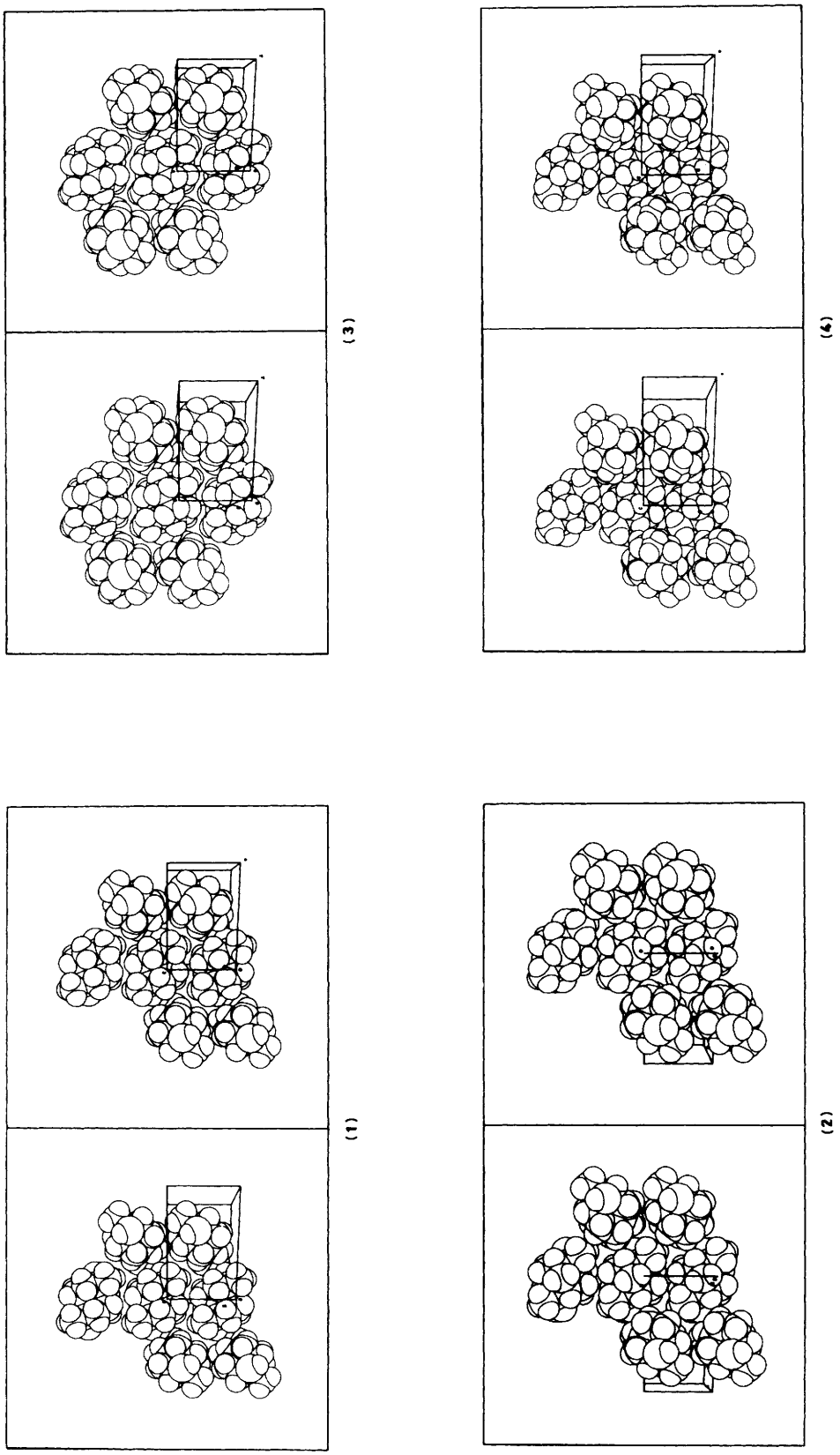

Figure 8. Stereopair pictures of the crystal structures of (**1**)—(**4**) at van der Waals volume, viewed towards the *anti* face of the tube, with molecules of the *syn* faces on both flanks. The *c*-axis is vertical. The OH groups can be recognised as the larger spheres with a single hydrogen atom.

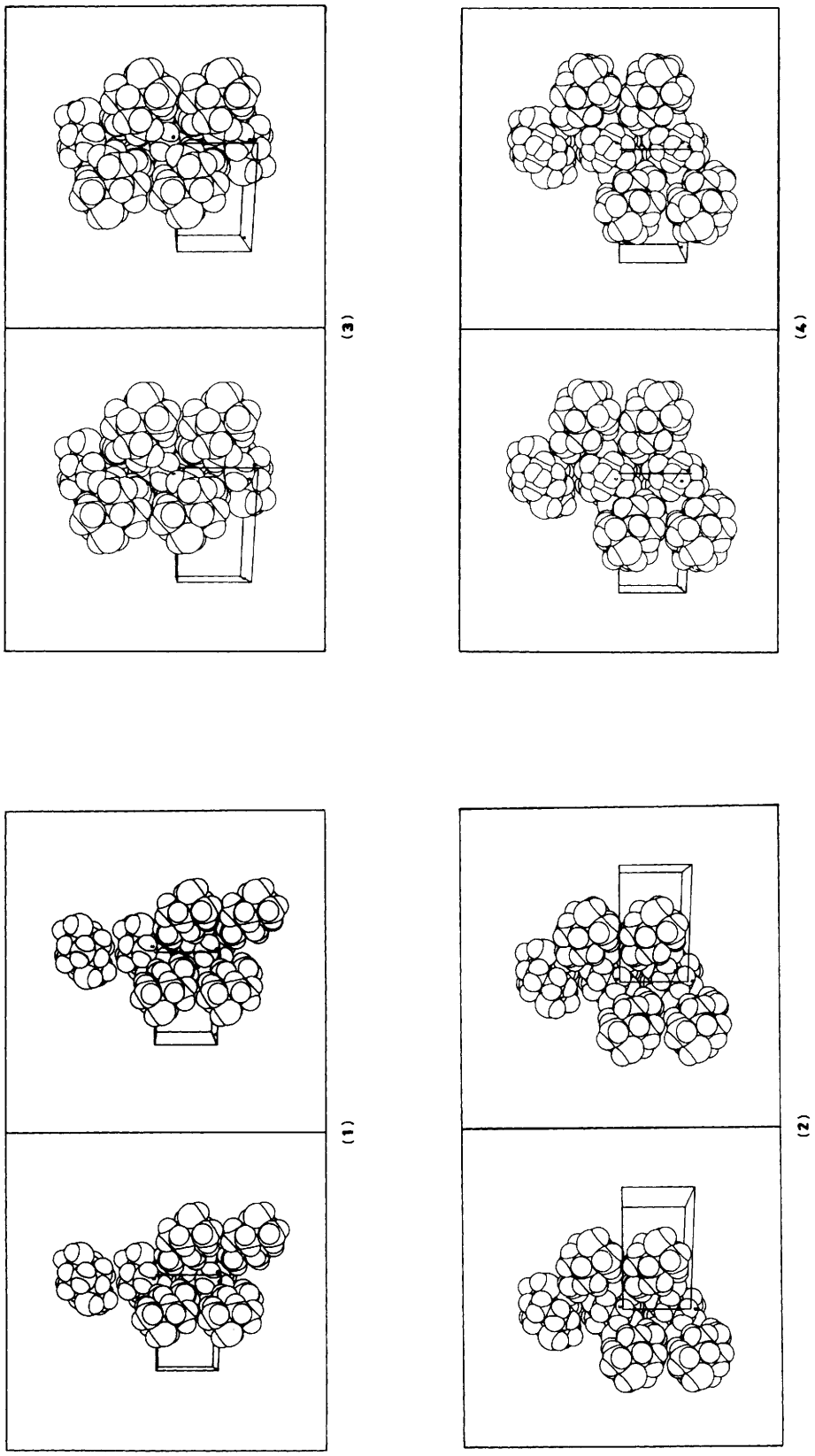

Figure 9. Stereopair pictures of the crystal structures of (1)—(4) at van der Waals volume, viewed towards the *syn* face of the tube, with molecules of the *anti* walls on both flanks. The *c*-axis is vertical

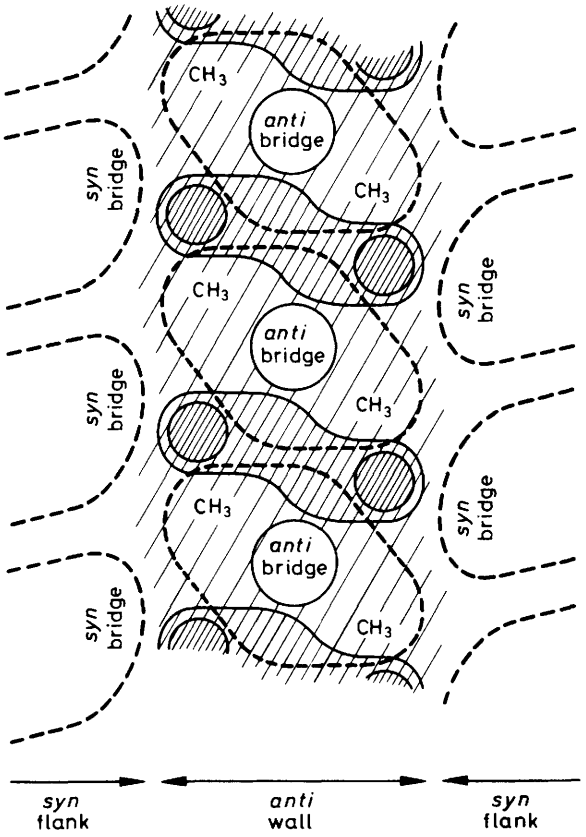

Figure 10. Schematic representation of the general topology of the *anti* wall. Diol molecules are outlined by broken lines. The locations of the protruding *anti* bridge and the methyl groups are marked. The degree of cross-hatching is proportional to the depth into the wall accessible to guest species.

the *syn* wall, and comparative analysis of the four structures is made in terms of the shape of the *anti* wall and of its *syn* wall flanks. The relevant stereodiagrams in Figure 8 show the same shape and pattern of indentations. The topological features of this general pattern are shown in Figure 10. The *anti* bridge protrudes from the wall in (**2**), (**3**), and (**4**), but because this bridge repeats at *c ca.* 7 Å there is substantial volume available between the *anti* bridges. A region of moderate depth extends over the remainder of the *anti* face, *including* the methyl groups. A deeper bent crevice extends across the wall, straddling the two-fold axes between the diol molecules, and contains even deeper tunnels which extend *through* the wall.* These tunnels are of insufficient size to accept guest termini, but the lateral crevices are in all cases sufficient to accommodate CH_3 ends or CH_2/CH edges of guest molecules. The significant result here is that (**3**) is not less capacious than the others in this regard.

The molecules in the flanking *syn* walls are situated such that the *syn* bridges protrude over the tunnels in the *anti* wall, and the crevices in the *syn* wall extend laterally from the methyl substituents in the *anti* wall, as shown in Figure 10. In fact the only barrier to guest movement between the crevice in the *anti* wall and the crevice in the *syn* wall without entering the unobstructed central region of the tube is that due to the methyl substituents.

In (**1**) and (**3**) the *syn* flanks are widely separated across the *anti* wall [see (**1**) and (**3**) in Figure 8] and as a corollary the views in Figure 9 of the *syn* walls in (**1**) and (**3**) appear as narrow crevices with encroaching *anti* flanks. Corresponding stereodiagrams show that for (**2**) and (**4**) the *anti* walls are more closely flanked and the *syn* walls are less closely flanked than in (**1**) and (**3**).

Volumes for Guest Inclusion.—It is obvious from the stereodiagrams that the tubes in (**1**) and (**2**) are sufficiently voluminous to accommodate the ethyl acetate guest in a variety of positions and orientations. In (**3**) the cavities between the bridges along the *anti* wall and the cavities between the bridges along the *syn* wall all have appreciable volume, sufficient to accommodate the *chain* components of guests. Figure 8 shows that the methyl group on the *anti* face of (**3**) partially obstructs the connection between these two cavities, but nevertheless the sequence of cavities spiralling around the walls between the protruding bridges does provide substantial volume to guest species that could adopt a spiral chain conformation. The rigid triangular section of ethyl acetate would be more difficult to accommodate, but our analysis of the stereodiagrams and of cross-sectional slices through the tube indicates that ethyl acetate could fit tightly into the host structure. In (**4**) the maximum diagonal of the unobstructed cross-section[1] of the tube is 8.4 Å (the minimum diagonal is 5.5 Å), while the van der Waals diameters of the potential guest, benzene, are *ca.* 7.0 Å for 1,4-hydrogen atoms and *ca.* 6.6 Å for 1,3-hydrogen atoms. Therefore the host tube should be sufficiently large to accommodate benzene guest molecules, aligned parallel to the tube axis. Six-fold disorder of the orientation of the guest plane around the tube axis is possible.

Summary and Conclusions.—In the family of four host structures described here there are variable and invariant geometrical features.

Significant constant factors are the separation of the key C–OH functions, and the relative orientation of these two functions. Thus, the diols as spine connectors are essentially invariant. A third constant factor is the methyl substituent,† while a fourth is the pitch of the hydrogen-bond helical spine.

Geometrical variation occurs in the *a* repeat lengths of the trigonal lattice, in the shapes and the bulk of the diol bridges which form the walls of the tubes, and in the rotational orientations of the hydrogen-bonded spines. This latter variation is alternatively expressed in terms of the positions of the diol connectors along the two-fold axes.

Causative factors can be recognised in this series of four diols, and incorporated in predictive structural hypotheses. The variable displacement of the diol molecules along the two-fold axes is attributed to repulsive interactions between the diol substituent (methyl) and the *syn* bridge atoms of contiguous diol molecules in the tube walls. The diol displacements and *a* variations due to this repulsion cause elongation of the hydrogen bonds, an elongation which correlates with decreasing m.p. for the crystalline diol. The shorter hydrogen-bond distances O - - - O = 2.81 and 2.84 Å in (**1**) and (**3**) occur in crystals with higher melting points (191 and 247 °C); the longer O - - - O distances (2.98 and 3.08 Å) occur in crystals (**2**) and (**4**) with lower m.p.s of 148 and 147 °C, respectively. This leads to the hypothesis that, in order to maintain a stable helical tubuland crystal structure, the *molecular* geometry of the host diol should be designed to minimise this particular interaction.

The same factor affects the cross-sectional size of the tubes.

* Figure 8 [(**1**) and (**3**)] shows that the crevice extends completely through the wall in (**1**) and (**3**), *i.e.* there is no van der Waals contact between host molecules along *c*.

† We have already reported[3] the effects of variation of this substituent on the bicyclic diol framework of (**1**).

The tube shape is determined by the bridges on both *syn* and *anti* faces of the diol.

The pitch of the hydrogen-bonded spine in the helical tubuland crystal structure must be related to the thickness of the host diol molecule as stacked along *c*. This dimension of the host molecule is not a variable in the current series. However, the possible range of this quantity can be estimated from the geometry of the hydrogen-bonded spine. The O---O distance d and the O---O---O angle α are related to the pitch, $3p$, of the trigonal spine helix by $p^2 = d^2[1 - (4/3)\cos^2(\alpha/2)]$. At the upper end of the range of pitch, $\alpha = 140°$, $3p = 2.756d$, *or* $3p = 7.99$ Å at $d = 2.9$ Å; at the lower end of the range, $\alpha = 90°$, $3p = 2.12d$, or $3p = 5.52$ Å at $d = 2.6$ Å. Thus it appears unlikely that the trigonal helical tubuland structure type could be maintained by diols with a stacking thickness differing by more than ± 1 Å from 7 Å. This is the limitation of the compression or elongation of the springs in the coiled-spring mattress analogy introduced for this structure type at the outset.

Finally we speculate that the length of the diol connector between the spines could be increased without contravention of any of the evident principles for this structure type. Such elongation would dramatically increase the size of the tube, and reduce the density of the host crystal. The question of upper limit to this lattice expansion by diol elongation is the subject of continuing investigations.

Acknowledgements

The support of the Australian Research Grants Scheme is gratefully acknowledged.

References

1 I. G. Dance, R. Bishop, S. C. Hawkins, T. Lipari, M. L. Scudder, and D. C. Craig, preceding paper.
2 E. Weber and H.-P. Josel, *J. Incl. Phenom.*, 1983, **1**, 79.
3 R. Bishop, S. Choudhury, and I. G. Dance, *J. Chem. Soc., Perkin Trans. 2*, 1982, 1159.

Received 3rd *September* 1985; *Paper* 5/1511